Estuarine Management and Technologies Journal

Estuarine Management and Technologies 1(1): 19–37 (2024)
DOI: 10.3897/emt.1.120413

Research Article

Estuary fluvial flooding: the example of the watercourse Miljašić jaruga in the town of Nin (Croatia)

Igor Ljubenkov[1], Dijana Oskoruš[2], Josip Rubinić[3], Ivan Peša[4], Jovan Papić[5]

1 *Water Development Ltd., Split, Croatia*
2 *Faculty of Geotechnical Engineering, University of Zagreb, Varaždin, Croatia*
3 *GEO-5, Rovinj, Croatia*
4 *Croatian Waters, VGI Zadar, Zadar, Croatia*
5 *Faculty of Civil Engineering, Ss. Cyril and Methodius University in Skopje, Skopje, Republic of North Macedonia*

Corresponding author: Igor Ljubenkov (iljubenkov@gmail.com)

Abstract

The Miljašić jaruga is one of the most important watercourses in Zadar County (Dalmatia, Croatia). The total length of this area is approximately 16 km, with an associated topographic catchment of approximately 191 km^2. The downstream portion of the stream is influenced by the sea (estuary).

The hydrological regime of the Miljašić jaruga is strongly influenced by climatic features; therefore, for most of the year, there is an outflow of catchment waters, whereas in the summer dry months, the river bed is mostly without outflow. It is also common for extreme precipitation to occur after a long dry period, resulting in sudden increase in water levels and flash floods.

One such extreme event occurred on September 11, 2017, when a severe storm followed by heavy rain affected Zadar and its hinterlands. On that occasion, approximately 240 mm/m^2 fell in Zadar over a period of 6 h, with an intensity of up to 70 mm/m^2/h. Such extreme rainfall activated violent and torrential runoff, flooding, and damage in the entire catchment area of the Miljašić jaruga, particularly in the most downstream part of the basin, in the area of the estuary and the town of Nin. Numerous infrastructural and communal facilities have been damaged, including the Nin Salt Works.

This paper presents the hydrological analysis of a flash flood event in the Miljašić jaruga estuary. A hydrological series of 26 and 27 years were compared, whereas the longer series include historical flood, using three distributions: normal, log-normal and Gamma. The relevant hydrological parameters (water levels and flows) used for dimensioning the flood defense system show great variability depending on the available data (time series) and calculation methodology. For example, variation of flow rate reached 41 m^3/s for 100-year high waters, that is, from 60 m^3/s (n = 26, normal distribution) to 101 m^3/s (n = 27, log-normal distribution). In engineering practice, the unreliability of the estimation of statistical quantities should be considered to improve the effectiveness of flood defense systems. The rehabilitation and reconstruction work conducted after a flood on hydrotechnical structures (embankments) in the estuary area is described. In addition, there is a need for adequate water management across the entire basin, such as the construction of retention and barriers, which would increase the level of flood protection in the most downstream parts, i.e., the estuary.

Key words: Croatia, embankment, estuary, flash flood

OPEN ACCESS

Academic editor: Joan Cecilia Casila
Received: 6 February 2024
Accepted: 23 May 2024
Published: 7 June 2024

Citation: Ljubenkov I, Oskoruš D, Rubinić J, Peša I, Papić J (2024) Estuary fluvial flooding: the example of the watercourse Miljašić jaruga in the town of Nin (Croatia). Estuarine Management and Technologies 1: 19–37. https://doi.org/10.3897/emt.1.120413

Copyright: © Igor Ljubenkov et al.
This is an open access article distributed under terms of the Creative Commons Attribution License (Attribution 4.0 International – CC BY 4.0).

Introduction

Estuaries are generally exposed to the risk of flooding caused by the interaction of several potential triggers such as high astronomical tides, storm surges, waves, and large fluvial flows.

Floods in estuaries and coastal areas can be divided into the following types: (a) fluvial, (b) tidal, (c) fluvio-tidal, and (d) storm surge. The dominance of a specific flood driver depends on its location (Bevacqua et al. 2019; Harrison et al. 2021; Meslard et al. 2022).

Because many people live and work in coastal areas, deltas, and estuaries, numerous economic activities have taken place there. For this reason, floods in these areas are of great concern to residents. This has been shown by numerous previous floods in estuaries worldwide, which have caused great losses with human casualties, and damage to infrastructure and the environment. In the future, in relation to climate change, the risk of estuary flooding will increase due to the rise in sea level, and the increased intensity/duration of precipitation, leading to increased intensity of fluvial runoff.

In this study, a fluvial flood of a Croatian estuary located in the central part of the eastern Adriatic coast was analyzed (Fig. 1). Several Croatian rivers flow into the Adriatic Sea and a large number of smaller watercourses (Fig. 1). Although each estuary is specific in its own way, all estuaries in Croatia share a common environment: the karst area (Bonacci 1987; Kresic 2013; Bonacci 2015). Flash floods are characteristic of karst areas because of their geological and hydrogeological characteristics, which enable relatively fast interactions and dynamics of surface and underground waters (Bonacci et al. 2006; Kresic 2013).

In the Adriatic Sea, fluvial flooding dominates owing to the strong orographic influence. In general, short-term intense precipitation is the main driver of flood processes in this area, with morphological conditions having the greatest influence. The most pronounced influences are proximity to the sea and topography, that is, the spread of mountain massifs higher than 1,000 m in the immediate vicinity of the coast. Rivers have a dominant influence on Croatian estuaries and simultaneously represent the upstream boundary conditions of the estuary. In contrast, the downstream boundary condition is the sea, whose influence in this area is weaker owing to the relatively small amplitudes of tidal movements. In the southern part of the Adriatic, the tidal movement rarely exceeds 40 cm, whereas, in the northern part, it reaches 1 m. In narrow channels and bays, tides can significantly rise during severe storms. Sea changes are of a mixed type, which means that they have a half-day rhythm during the full and new moons and a daily rhythm during the first and last quarters. The amplitudes are also irregular.

The combination of high sea levels and intense precipitation in river basins can further increase water levels in estuaries, thus increasing the risk of floods (fluvio-tidal floods). However, such combinations should be analyzed separately. Rising sea levels and extreme climatic conditions (IPCC 2023) will increase inundation hazards in estuaries. Considering the complexity of this system, flood risk assessment in estuaries and coastal areas requires specific approaches that are not identical to the classical analyses of river floods (Bonacci 1987; Martin-Vide et al. 1999; Bonacci et al. 2006; Camarasa-Belmonte 2016). Flood risk estimates are traditionally based on univariate flood frequency

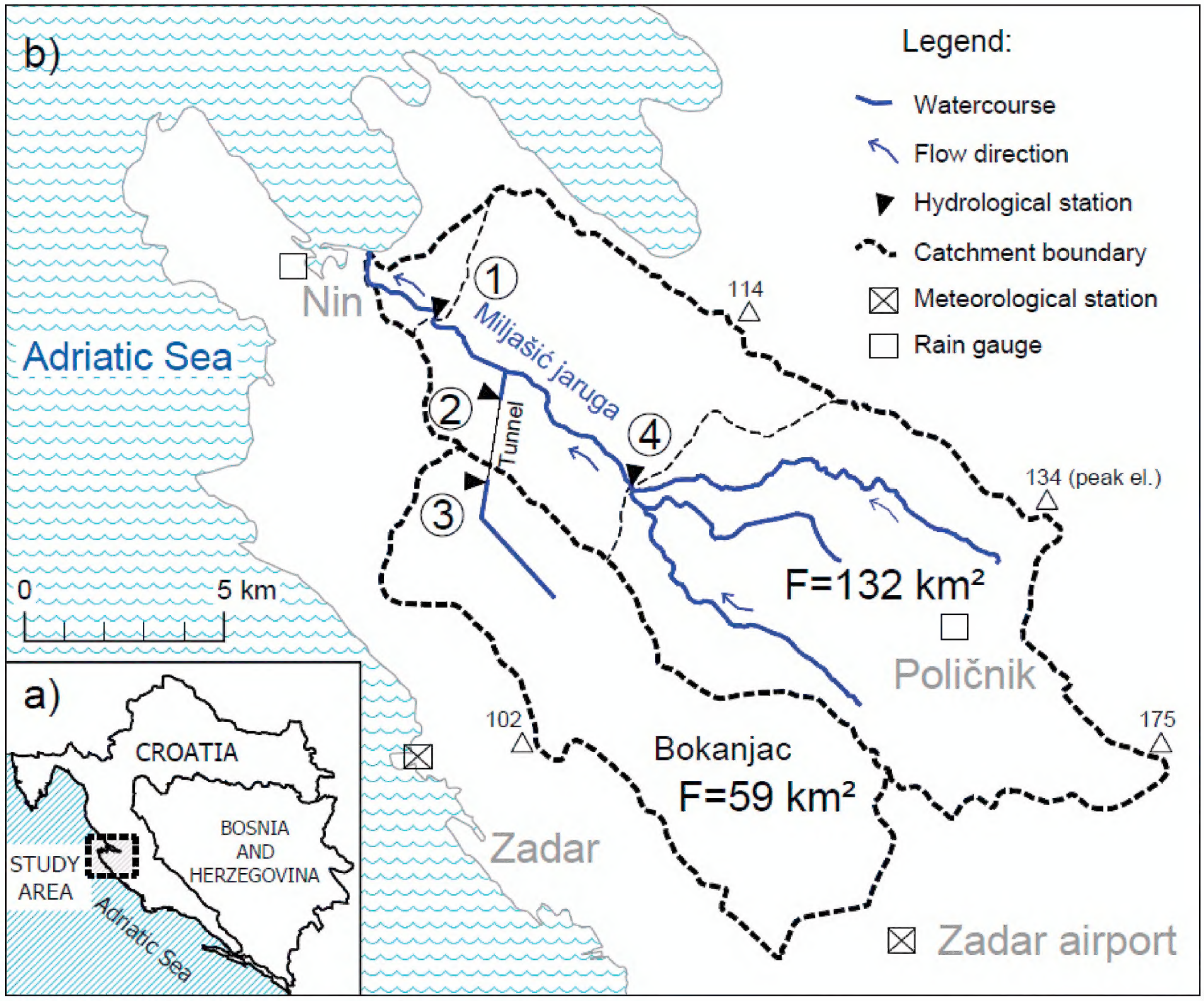

Figure 1. Map of catchment area of the Miljašić jaruga.

analysis, i.e., fitting distribution functions to ordered sequences of observed flood peaks (often annual maximum flow) and applied for assessment of riverine flood hazard (Lóczy et al. 2012; Ljubenkov et al. 2023). Generally, regarding the coastal-estuarine regions flooding risk approach, bivariate (multivariate) flood frequency analysis could be applied (Petroliagkis et al. 2016; Harrison et al. 2021; Lu et al. 2022). In our case, because the cause of the flood was exclusively inflow from the basin, a classic approach was applied. However, future research should consider the possibility of multivariate flood frequency analysis for estimating coastal-estuarine flooding risks.

The aim of this study was to improve the understanding of estuary flooding processes in a general sense. It also indicates possible unreliability in the assessment of input, meteorological, and hydrological data, which we used for designing the hydrotechnical systems. Furthermore, the research served to define the relevant parameters for the construction or reconstruction of the flood defense system in this watercourse. There is a need for further development of the water management system in the entire basin, which would also achieve greater security in the estuary area. An example of this watercourse is a karst flood that arises quickly, making it difficult to provide adequate warnings or preventive measures.

Study area

The Miljašić jaruga estuary is located in the central part of the eastern Adriatic coast. The Adriatic Sea (138,600 km^2) separates the Italian Peninsula from the Balkan Peninsula. The Adriatic is the northernmost arm of the Mediterranean Sea, extending from the Strait of Otranto (where it connects to the Ionian Sea) to the northwest and to the Po Valley (Italy). Countries that share an Adriatic coast are Albania, Montenegro, Bosnia and Herzegovina, Croatia, Slovenia, and Italy.

Unlike the western Italian coast, which is lower and sandy-muddy, the eastern coast of the Adriatic Sea is a Dinaric karst. The Croatian coast was formed from Adriatic carbonate platform, limestone. It is a large area of the sea where the shells of marine organisms accumulate. For millions of years, they settled at the bottom, and the pressure of the sea and their own weight compressed them into a compact rock. When the African Plate collided with the Eurasian Plate, a large part of the platform was lifted into the Dinarides, however, a part remained under sea. Along the Croatian coast and close hinterland, a series of mountains (Učka, Velebit, Dinara, Mosor, and Biokovo) with peaks over 1,000 m above sea level with a typical Dinaric direction of extension northwest-southeast have been established. Therefore, the estuaries of Croatian rivers are often cut deep into limestone, which is the dominant rock on the eastern coast of the Adriatic (Bonacci 2015; Ljubenkov and Haddout 2024).

The Miljašić jaruga catchment has a well-developed hydrographic network of surface and underground watercourses. The direct catchment (132 km^2) comprises a low and slightly undulating plain that is slightly inclined from the eastern edge of the catchment towards the northwest. The Miljašić jaruga begins its course at an altitude of approximately 88 m above sea level and, after 16 km, it ends by flowing into the sea approximately 900 m northeast of the center of the old town Nin.

The main tributaries of the Miljašić jaruga (Fig. 1) in its upper part of the catchment are the shorter torrential streams, Menjača and Briševačka jaruga. In addition, the Miljašić jaruga receives water from the area of Bokanjac in its middle course, through a hydrotechnical tunnel (approximately 2 km long). It is an indirect part of the catchment with an area of 59 km^2 (Fig. 1). Bokanjačko blato (Bokanjac) is a natural depression in which, in the past, lake water remained for most of the year. To encourage the development of agriculture, hydromeliora-

tion work was performed and the lake was drained by constructing a tunnel.

Geologically, the catchment area is dominated by Eocene limestone and marl, which mostly occur in narrow strips along the edges of the syncline, whereas the Eocene flysch layers extend beyond the edges of the syncline and are rich in clay. Wide valleys are typically deeper covered by marl and sandstone. Such geological structures determine the different hydrogeological features of the basin itself, that is, different degrees of water permeability.

The aforementioned estuary or the most downstream section of the 1.5 km long stream is directly influenced by the sea. In the past, the mouth of the river was located in an urban area in the town of Nin, and its core was formed on its alluvium. At the beginning of the 20th century, the river mouth was regulated, and it was moved 1.5 km to the north of the current route, which created conditions for the reconstruction and expansion of the salt pan in the immediate hinterland of Nin. The exploitation of salt in this location dates back more than 1,500 years. However, in the middle of the 20th century, modern salt works were

established, covering 55 ha (Fig. 2). Traditionally, salt is produced in numerous pools. Owing to favorable natural and climatic conditions (sea water, sun, and wind), salts of excellent quality are obtained. The salt pan pools on the eastern side are protected by an embankment from the high waters of the Miljašić jaruga. The route of the embankment follows the current bed of the Miljašić jaruga. With the construction of the embankment, water was directed exclusively towards the north, whereas the old flow route (bed) was abandoned.

The occurrence of extremely high water levels, which were recorded on September 11, 2017, caused unprecedented flooding (Oskoruš et al. 2018). On that occasion, there was damage and partial collapse of the Miljašić jaruga embankment. The average and maximum annuals flow at the nearby hydrological station, Boljkovac, are 1 m^3/s and 28.5 m^3/s, respectively, whereas the maximum flow from the aforementioned flood was estimated at 112 m^3/s (Fig. 2).

The recorded maximum was partially mitigated by the overflow of flood water outside the riverbed upstream of the hydrological station. In the area of the estuary, on that occasion, there was an outflow of flood water through the watercourse bed in the northern direction, but also laterally over the embankment, with the outflow spilling over the salt pan basin and the old bed in the westerly direction towards the center of the town. This extremely high level of water caused great damage in the lowland section of the stream, the wider area of the estuary, and in the upstream parts of the Miljašić jaruga catchment.

Climatic and hydrological conditions

According to Köppen's classification, the Dalmatian coast and islands have a Mediterranean climate with dry and hot summers (*Csa*), characterized by a late autumn maximum of precipitation, whereas summers are dry (DHMZ 2008). The average temperature of the warmest month is > 22 °C, and that of the coldest month is > 4 °C.

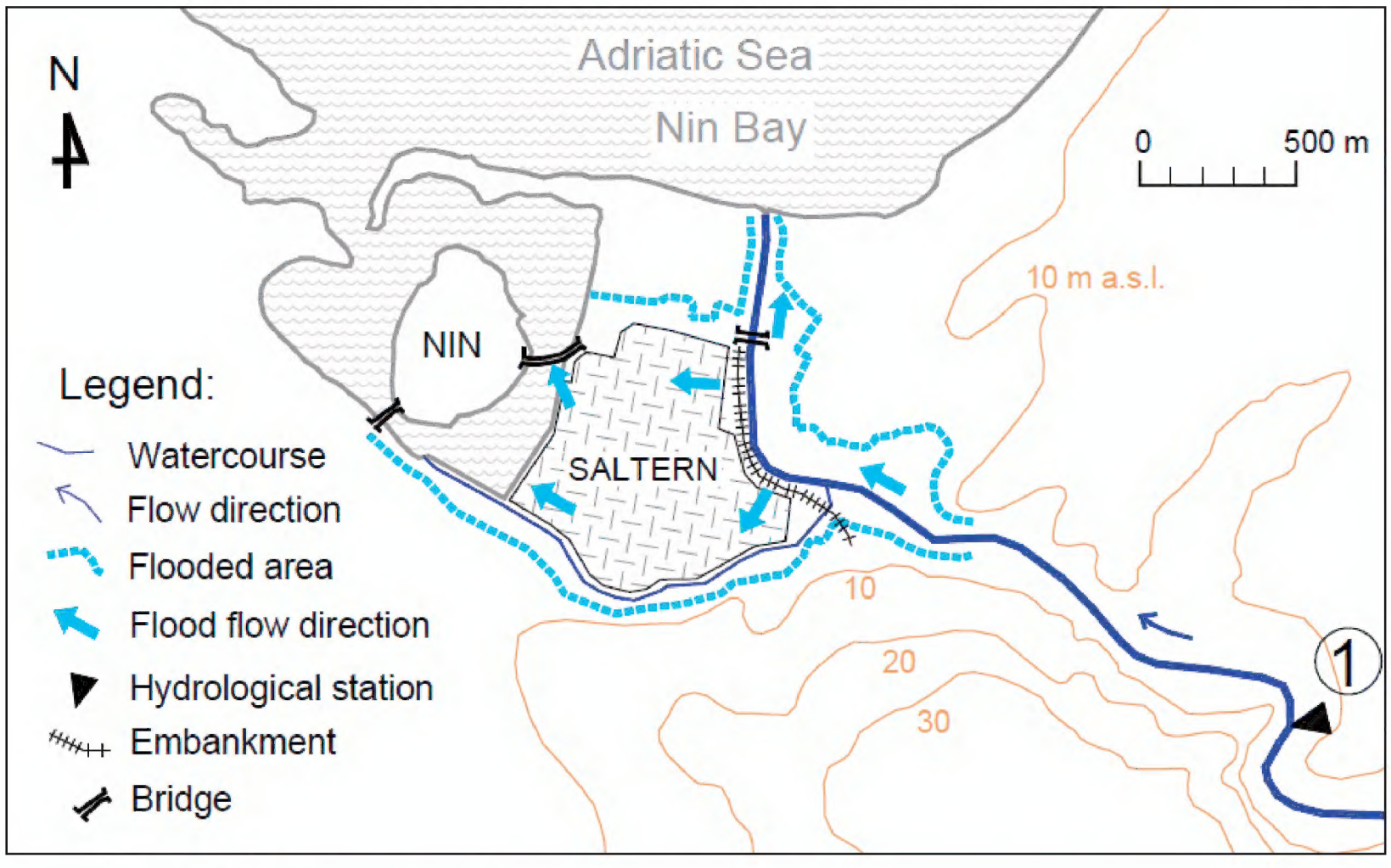

Figure 2. Map of the Miljašić jaruga estuary.

In this area, two meteorological stations, Zadar and Zadar Airport, operate, where all climatic elements are monitored and/or registered continuously over 24 h (Fig. 1). On addition, two rain gauges are in operation: Nin and Poličnik, where the amount of precipitation is measured every day at 7 a.m. official (Central European) time (Table 1). Fig. 3 shows the characteristic values of monthly precipitation for Zadar station in a 10-year period (2013–2022). On average, the rainy months were September and November, with 146 mm and 143 mm of precipitation, respectively. The September maximum from 2017 was clearly visible, at 460 mm/month when an extreme flood appeared.

Table 1. Basic data of rain gauge stations.

Station name	Type	Latitude, Longitude	Elevation
Zadar	Meteorological	44°7'48"N, 15°12'21"E	5 m
Zadar airport	Meteorological	44°5'42"N, 15°21'12"E	82 m
Nin	Rain gauge	44°14'30"N, 15°10'37"E	4 m
Poličnik	Rain gauge	44°10'1"N, 15°22'38"E	110 m

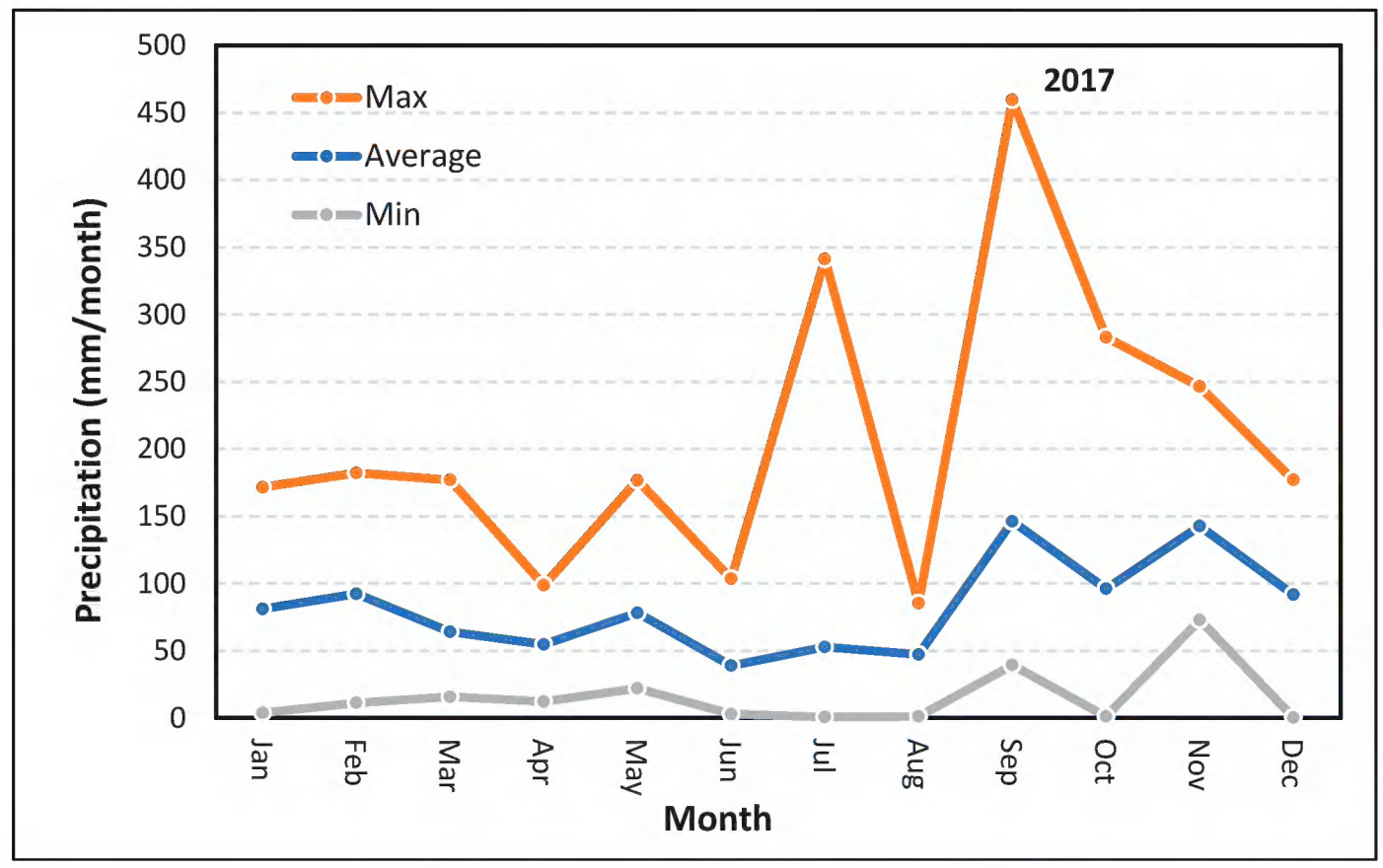

Figure 3. Characteristic values of monthly precipitation (Zadar, 2013–2022).

Rainfall during the flood event

Table 2 shows daily amounts of precipitation for September 10, 11 and 12, 2017. The highest values were recorded on September 11, with a maximum in Zadar (284 mm). The total 3-day precipitation was > 300 mm at Zadar and Zadar Airport stations. Such large and intense precipitation caused extremely large and violent surface runoff and ultimately a historic flood, particularly in the most downstream part of the catchment. Interestingly, the precipitation in Nin on the mentioned days was small, almost negligible compared to other stations.

Fig. 4 shows the hourly precipitation values on September 11, registered at the Zadar meteorological station. The highest precipitation intensity (mm/h) was recorded early in the morning at 7 a.m. and 8 a.m. local time. The maximum hourly, 2-h, 3-h and 4-h precipitation was 70 mm, 137 mm, 170 mm, and 221 mm, respectively.

Table 2. Daily precipitation amounts (mm) (September 10–12, 2017).

Station	Sep 10, 2017	Sep 11, 2017	Sep 12, 2017	Total
Zadar	21	284.3	8.6	313.9
Zadar airport	74.2	279.6	11.8	365.6
Poličnik	0	208	21.6	229.6

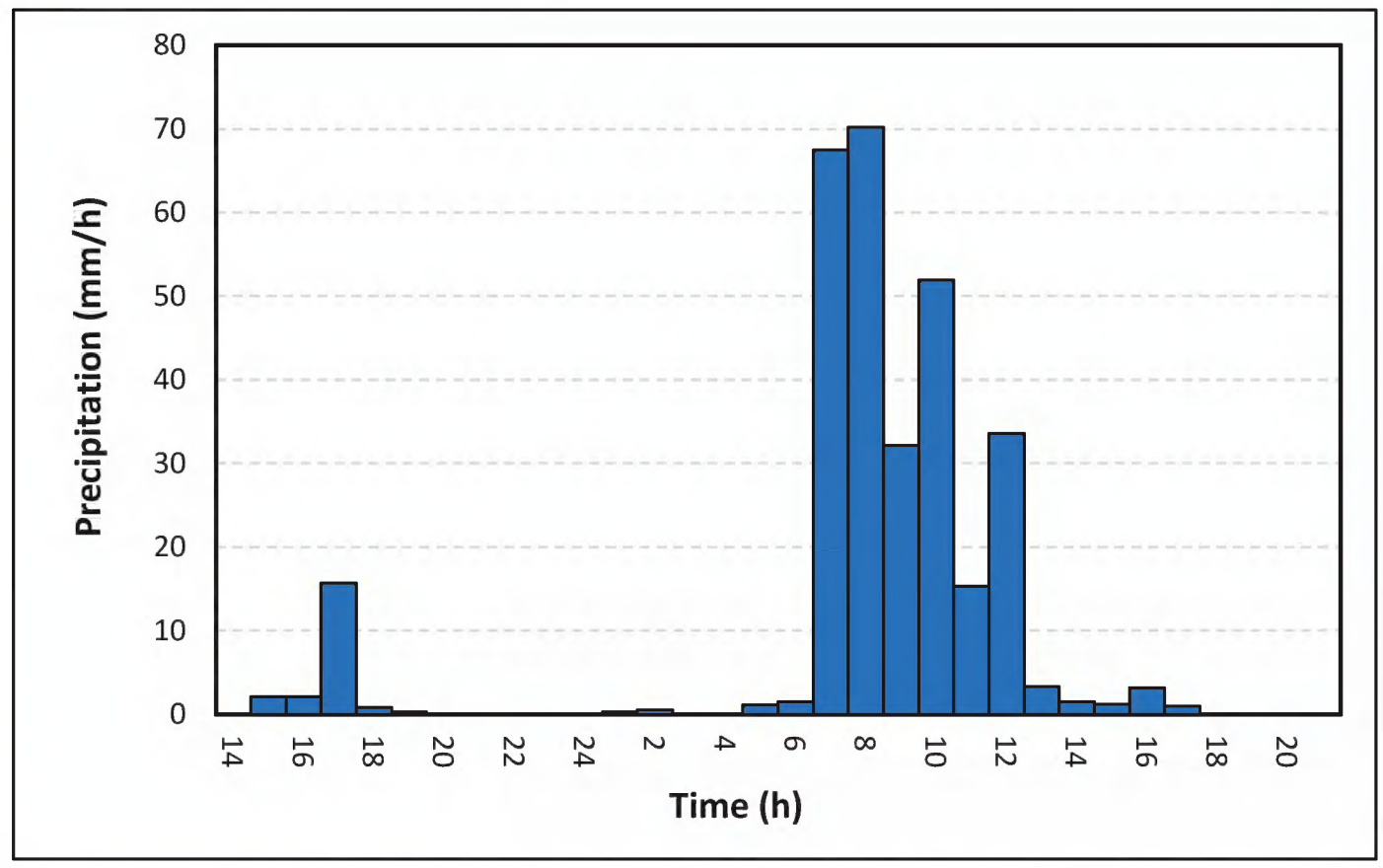

Figure 4. Hourly values of precipitation on September 10 and 11, 2017 (Zadar).

Fig. 5 shows the calculated rainfall depth-duration-frequency (RDF) curves for the Zadar ombrographic station (for 1961–2020) with a precipitation duration of up to 1 day (1440 min) and a return period of up to 100 years. Additionally, envelopes of the maximum registered precipitation were drawn, which mainly belonged to two extreme precipitation situations from 1986 and 2017. According to available data, the highest daily precipitation in Zadar was recorded on September 10, 1986 (357 mm), followed by September 11, 2017 (284 mm). As showen in Fig. 5, the maximum recorded precipitation exceeds the calculated values of the RDF curves for the 100-year return period for durations > 1 h (60 min). The greatest difference between the recorded and calculated values was for a duration of 4–6 h, when the measurements were significantly higher than the 100-year maximum precipitation. For example, the 4-h calculated precipitation for the 100-year period was 187 mm, whereas the 4-h precipitation was 221 mm in 2017.

Water level of the flood event

Hydrological measurements were conducted at four hydrological stations, two of which are located on the watercourse of the Miljašić jaruga: Poljaki and Boljkovac, whereas two are on the left tributary of the Miljašić jaruga, that is, on the drainage channel and tunnel of Bokanjačko blato (Table 3). Because these stations began operating in 1996, no earlier hydrological data were available. Fig. 6 shows the water waves registered at the aforementioned hydrological stations during the floods. In the Miljašić jaruga (stations Poljaki and Boljkovac),

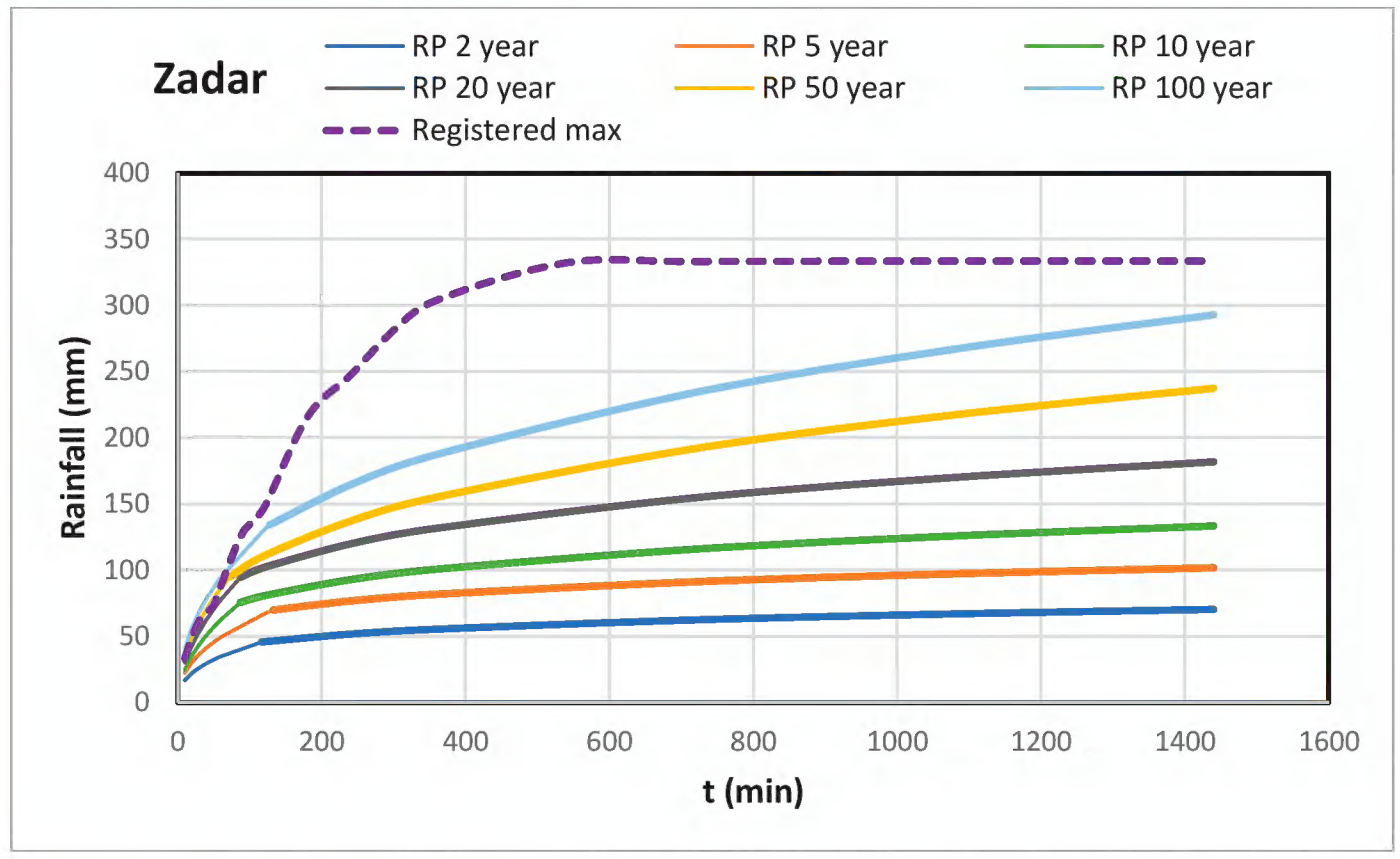

Figure 5. Rainfall depth – duration – frequency curves (Zadar, 1961–2020).

Table 3. Basic data of hydrological stations.

No.	Station name	Watercourse	Level "0" of the water mark	Min. water level	Max. water level	Start of work
In Fig. 1			(m a.s.l.)	(cm)	(cm)	(year)
1	Boljkovac	Miljašić jaruga	2.213	Dry	353	1996
2	Tunel izlaz	Bokanjačko blato	9.161	Dry	272	1996
3	Tunel ulaz	Bokanjačko blato	14.711	Dry	163	1996
4	Poljaki	Miljašić jaruga	25.022	Dry	367	1996

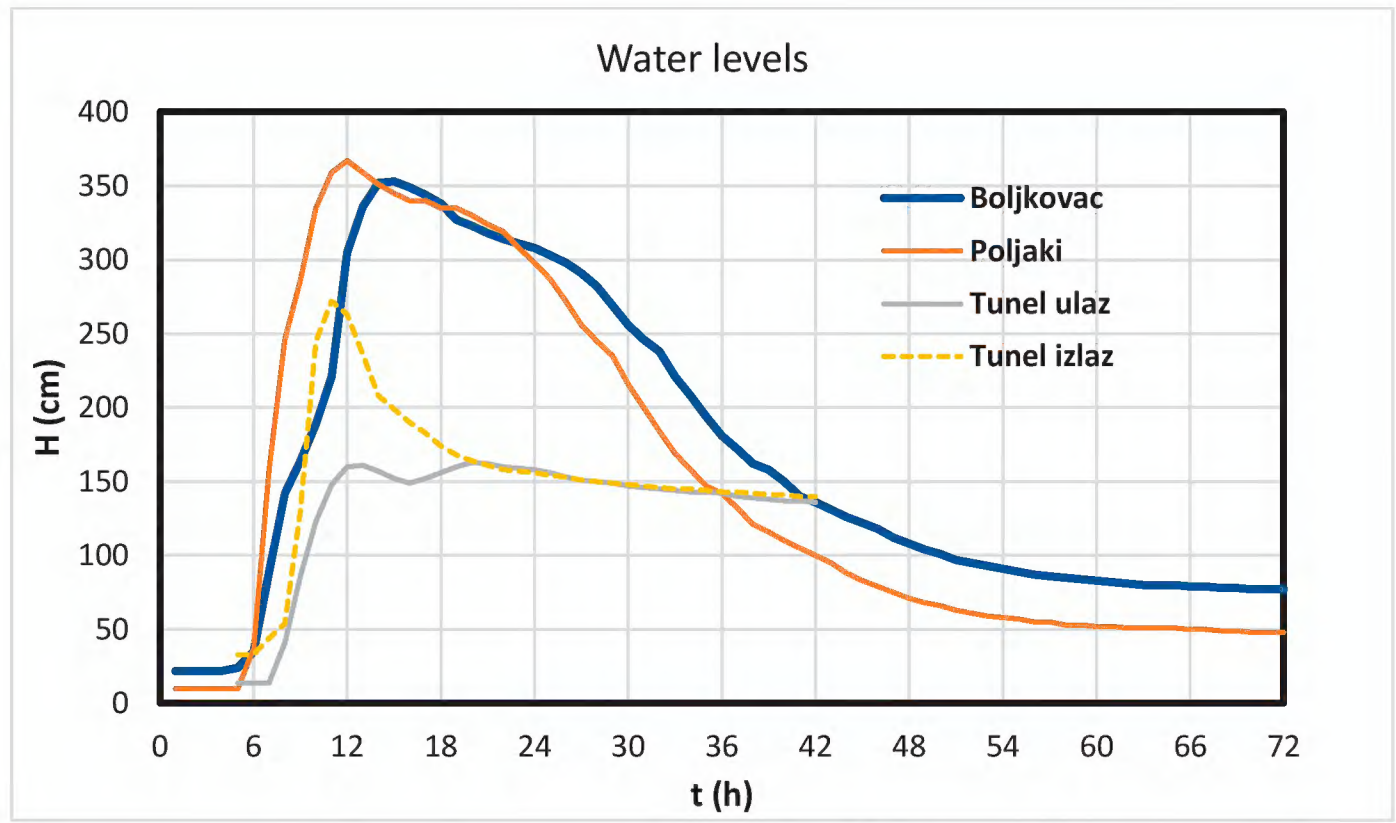

Figure 6. Water level recordings at hydrological stations (September 11–13, 2017).

the water level begins to rise from 6 a.m. The highest water level rise gradients (ΔH) were at 7 a.m. and 12 a.m. at the upstream (Poljaki, 121 mm/h) and downstream stations (Boljkovac, 84 mm/h), respectively. The peak of the flood water at Poljaki station was at 12 a.m. (367 cm), whereas it was 353 cm at 3 p.m. at Boljkovac station. This is the typical shape of a flash flood chart, with a large rise

in the water level over a relatively short time. For example, at the Poljaki station, the water level increased by 357 cm within 7 h. At the entrance to the tunnel, two peaks were recorded on the runoff level graph, owing to the influence of the tunnel, at 1 p.m. (H = 161 cm) and at 8 p.m. (H = 163 cm). On the downstream side of the tunnel, the maximum water level was at 11 a.m. (H = 272 cm), after which the water level continuously decreased (Oskoruš et al. 2018).

Discharge during the flood event

According to the extrapolated discharge curve of the Boljkovac station, the 2017 flood wave had a maximum flow of 112 m^3/s, and the total volume of flood water was approximately 10.6 million m^3. The maximum flow at the Poljaki hydrological station was 91 m^3/s and the total volume of water was approximately 7.7 million m^3. According to the data from the hydrological station Tunel izlaz, the inflow from the area of Bokanjac was 1.8 million m^3, with a maximum flow of 22.6 m^3/s. Fig. 7 shows runoff hydrographs. The time lag between the rainfall peak (8 a.m.) and discharge peak was 4 h for Poljaki station (12 a.m.) and 7 h for Boljkovac station (3 p.m.).

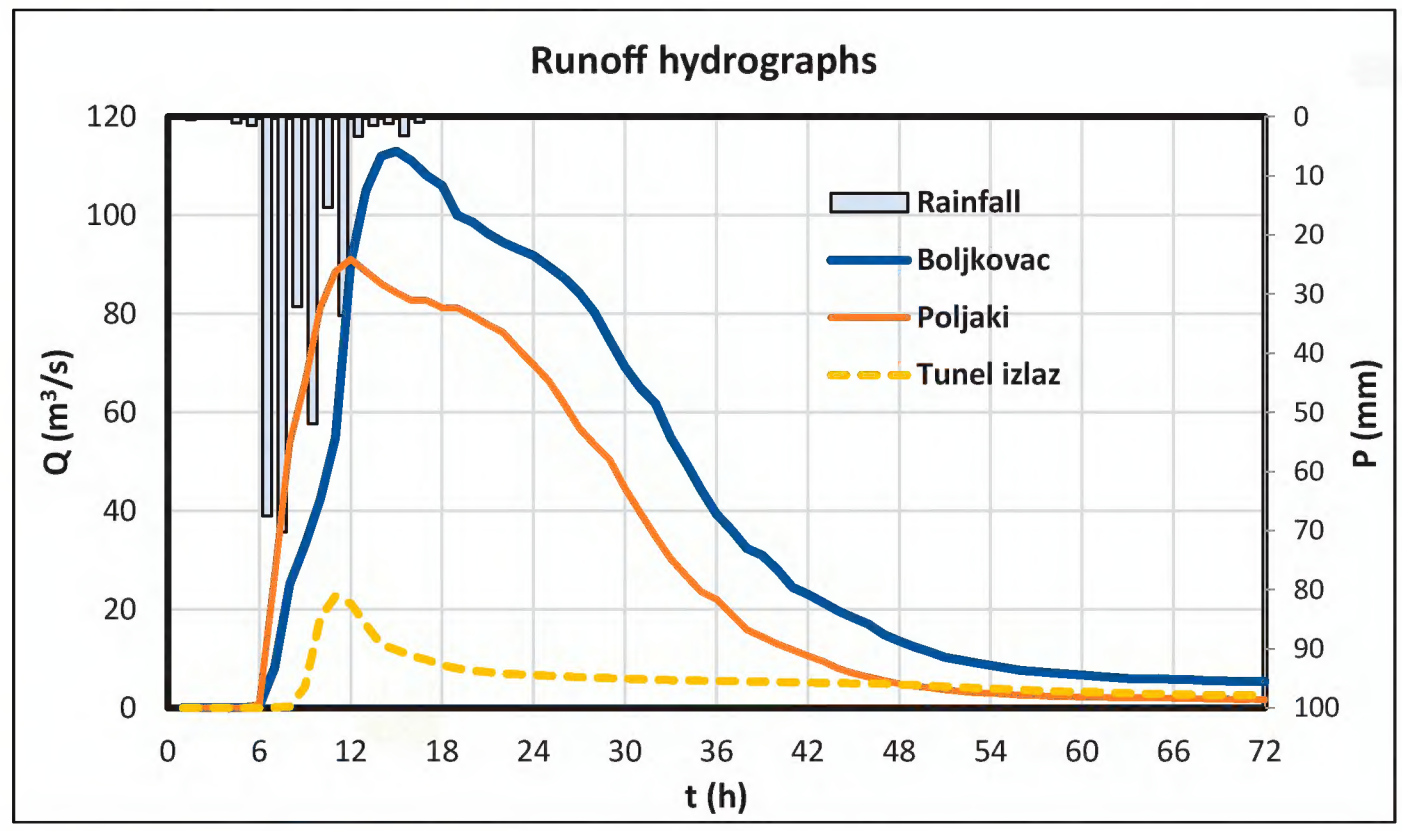

Figure 7. Runoff hydrographs (September 11–13, 2017).

The flow estimation for large water levels is based on extrapolated flow curves and may have a relatively large error. Therefore, the official maximum flows should be considered as the estimated quantities. Nevertheless, the specified values of the maximum flow and volume of water waves provide an order of magnitude of extreme hydrological phenomena that occur rarely.

From a hydrometeorological point of view, flash floods are best described as events characterized by large amounts of water in a short time. In general, the cause is extremely large amounts of precipitation, which, in combination with favorable conditions for surface runoff in relatively small watersheds, form flash floods. They occur immediately after a storm event, with a time lag in the maximum runoff of a few minutes to a few hours after a rain event. The term 'flash' means a sudden, rapid hydrological reaction. Flash floods are generally limited to basins with an area of several hundred square kilometeres or less. Therefore,

there are also time restrictions: response times do not exceed a few hours or are even shorter (Lóczy et al. 2012). Karst flash floods are a special type of flash floods related to the structural and hydraulic properties of a karstic systems (Bonacci et al. 2006; Marechal et al. 2008; Jourde et al. 2014; Ljubenkov et al. 2023).

Statistical analysis of large fluvial waters

Three theoretical distribution curves were used to analyze the probability of maximum annual water levels at the Boljkovac hydrological station: normal, log-normal, and Gamma (Mimikou et al. 2016). Compared with discharge data, level data can be considered more reliable than input data because the peak values of the annual maximum discharge are obtained by a large extrapolation of the discharge curve. Therefore, the discharge was estimated and not measured, in contrast to the water levels that were continuously recorded at the hydrological station (limnigraph). Hydrological data (annual maximum water levels) from 1996–2022 were considered (Fig. 8).

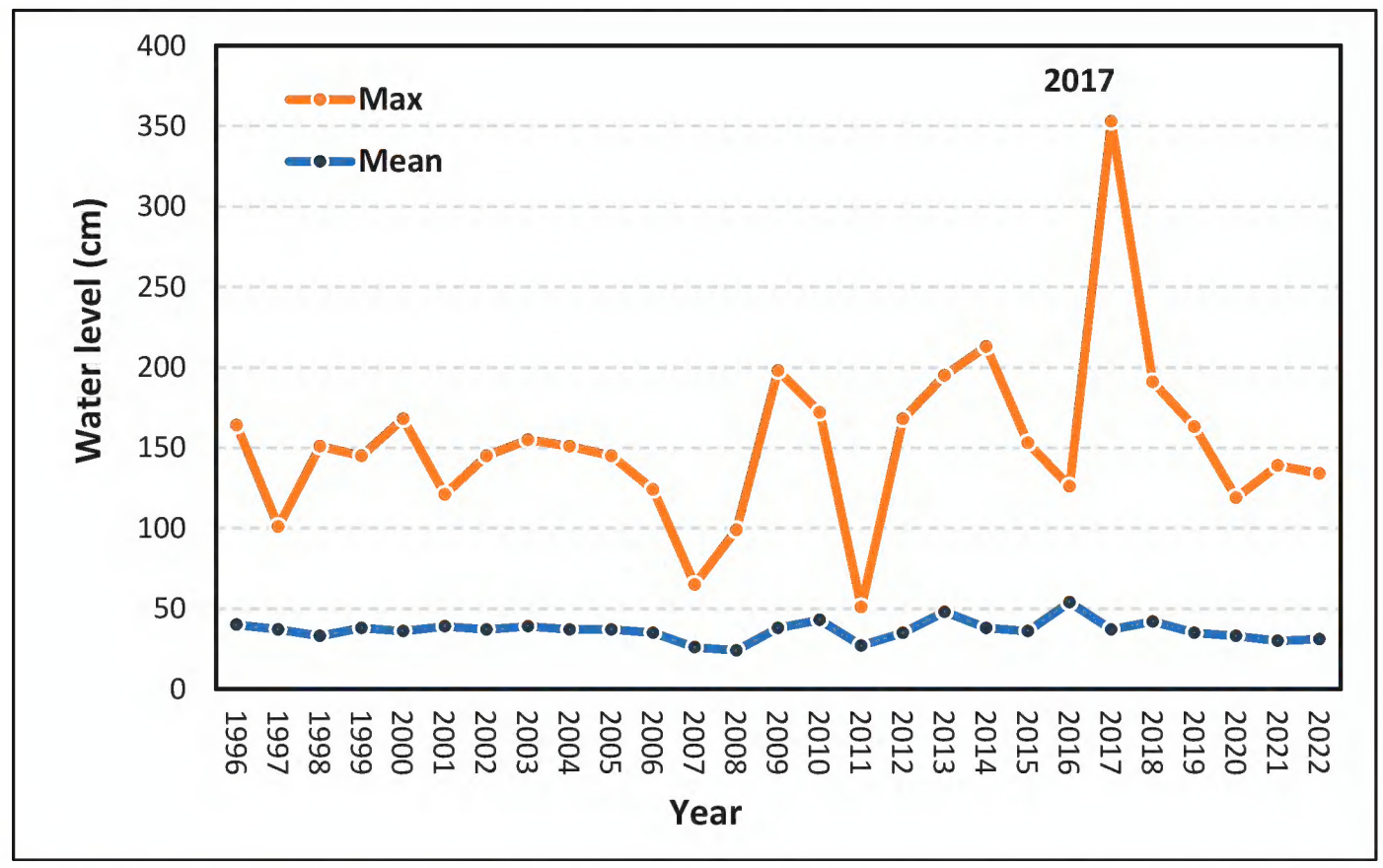

Figure 8. Series of the maximum and mean annual water levels (Boljkovac, 1996–2022, n = 27).

The general forms of probability density functions ($f(x)$) and cumulative distributions ($F(x)$) are

Normal distribution (*Gaussian distribution*)

$$f(x) = \frac{1}{\sigma \cdot \sqrt{2\pi}} \cdot e^{-\frac{(x-\mu)^2}{2\sigma^2}} \quad -\infty < x < +\infty \tag{1}$$

$$F(x) = P(X < x) = \frac{1}{\sigma \cdot \sqrt{2\pi}} \cdot \int_{-\infty}^{x} e^{\frac{(t-\mu)^2}{2\sigma^2}} dt \tag{2}$$

The parameter μ is the mean, whereas the parameter σ is the standard deviation.

Log-normal distribution

$$y = \ln X \; f(y) = \frac{1}{\sigma_y \cdot \sqrt{2\pi}} \cdot e^{-\frac{(y-\mu_y)^2}{2\sigma_y^2}} \quad 0 < y < +\infty \tag{3}$$

$$F(y) = P(Y < y) = \frac{1}{\sigma_y \cdot \sqrt{2\pi}} \cdot \int_0^y e^{-\frac{(y-\mu_y)^2}{2\sigma_y^2}} dy \quad (4)$$

In probability theory, a log-normal distribution is a continuous probability distribution of a random variable whose logarithm is normally distributed. Thus, if random variable *X* is log-normally distributed, then *Y* = *ln*(*X*) has a normal distribution. The parameters μ_y and σ_y are the mean and standard deviations of the *Y* variable, respectively.

Gamma distribution

$$f(x) = \frac{1}{\beta^{\alpha} \cdot \Gamma\alpha} \cdot x^{\alpha-1} \cdot e^{-\frac{x}{\beta}} \; 0 < x < +\infty \quad (5)$$

$$F(x) = P(X < x) = \int_0^x \frac{1}{\beta^{\alpha} \cdot \Gamma\alpha} \cdot t^{\alpha-1} \cdot e^{-\frac{t}{\beta}} dt \quad (6)$$

$$\Gamma(\alpha) = \int_0^{\infty} x^{\alpha-1} \cdot e^{-x} dx \quad (7)$$

where α and β are shape and rate parameters, respectively. $\Gamma(\alpha)$ is the Gamma function.

The parameter values of the distribution are listed in Table 4. Parameter values differed depending on the selected input data (n = 26 or 27). The probability density functions and cumulative distributions are shown in Fig. 9.

Table 4. Distribution parameters.

No.	Distribution	Parameters		n = 26	n = 27	Difference	Diff. %
1.	**Normal**	Mean	μ	144.46	152.19	7.73	5.2
		Standard deviation	σ	38.08	54.82	16.74	36
2.	**Lognormal**	Mean	μ_y	4.930	4.965	0.035	0.7
		Standard deviation	σ_y	0.322	0.364	0.042	12
3.	**Gamma**	Shape	α	14.393	7.708	6.685	60
		Rate	β	10.037	19.745	9.708	65

The agreement between the empirical and theoretical distributions was tasted using the Kolmogorov–Smirnov (K-S) test. The K–S test is used to determine whether a sample comes from a population with a specific distribution (Massey 1951; Drew et al. 2000). The theoretical distribution must be continuous (i.e., no discrete distributions such as binomial or Poisson distributions), and must be fully specified. The K–S test compares a known hypothetical probability distribution (e.g., a normal distribution) to the distribution generated by the input data (e.g., the empirical distribution function). The test statistic (*D*) is the largest distance between the empirical distribution (*Fn*(*x*)) and cumulative distribution (*F*(*x*)) of the hypothesized function, measured in the vertical direction.

$$D = max \left| Fn(x) - F(x) \right| \quad (8)$$

If D is greater than the critical value, the null hypothesis (H0) is rejected (Massey 1951; Drew et al. 2000; Mimikou et al. 2016). The hypotheses for the test are:

- Null hypothesis (H0): The data comes from the specified distribution.
- Alternate hypothesis (H1): At least one value does not match the specified distribution.

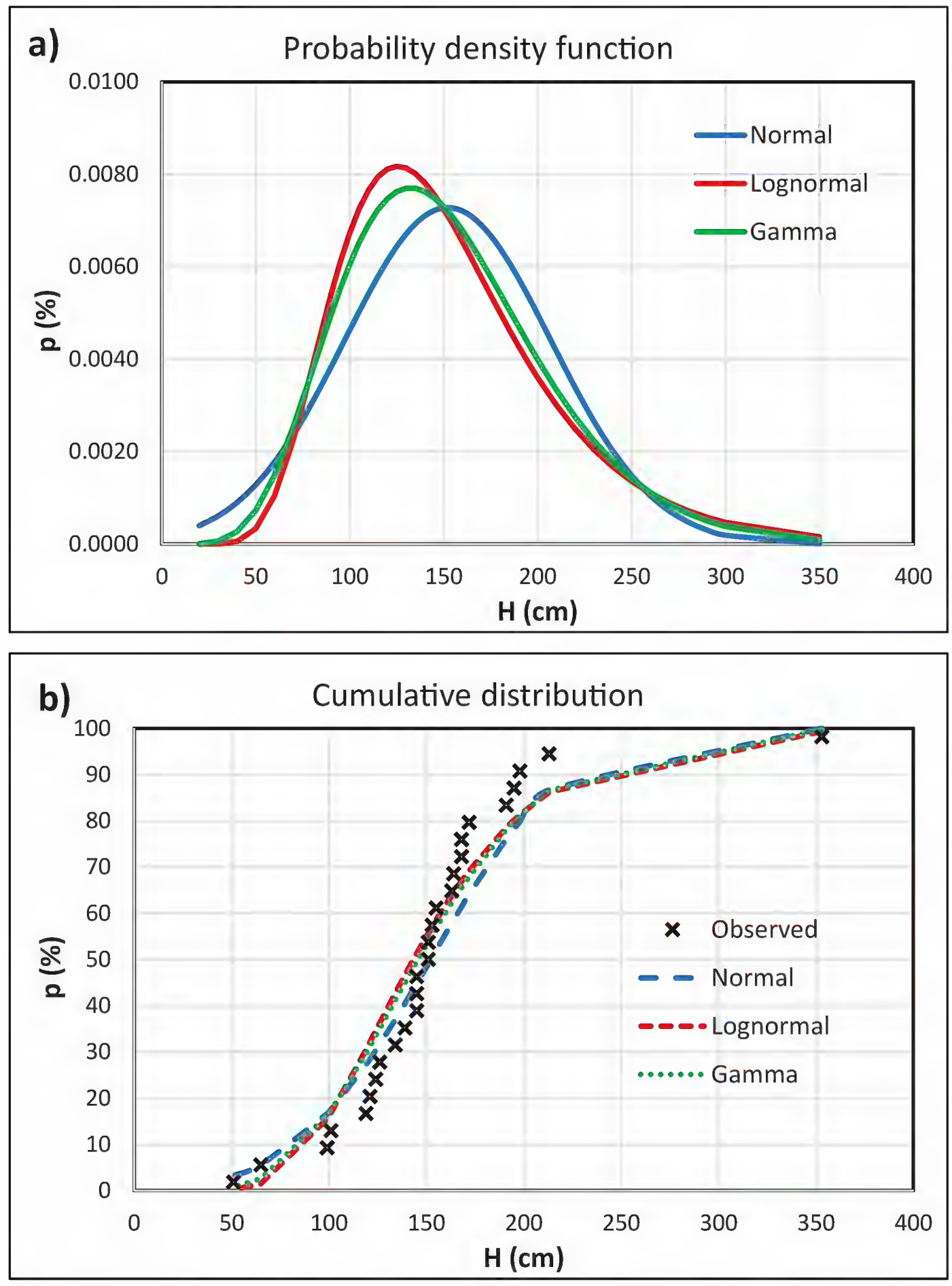

Figure 9. Comparison of distribution curves (Boljkovac, 1996–2022).

Results and discussion

In this case, all three distributions were statistically acceptable (K–S test). The Gamma distribution exhibits the best matching of the associated functions. Nevertheless, the results of the analysis of all three curves are presented, indicating the extent of data dispersion. In general, the starting series (up to 27 datasets) was relatively short, that is, not long enough for us to draw reliable conclusions about large water flows, for example, a return period (recurrence interval) of 100 years or more.

Table 5 shows the results of the statistical analysis, that is, the calculated levels of large water flows for return periods of 2–500 years. Comparing the selected distributions, the highest water levels were given by the log-normal distribution, followed by Gamma, and the lowest were given by the normal distribution. Comparing the input series with 26 or 27 dataset points, higher water levels gave a longer series (n = 27) because they also considered extreme flooding events. The table shows the differences in water levels for the different distributions and selected series. According to the above statistical estimates, the 2017 flood (H = 353 cm) had a return period of > 500 years, with a normal distribution. With the Gamma distribution, the corresponding return period was approximately 500 years, and with the log-normal distribution, it was slightly less than 200 years. Water–level dispersion was even greater with longer return periods. Comparing the input series with 26 (series of maximum annual water levels without 2017) or 27 datasets (series of maximum annual water levels 1996–2022), for example, the 100-year water level differences varied from 39 cm to 60 cm. Based on the conducted K–S tests, we consider the Gamma distribution to be relevant in this case; therefore, the characteristic levels of high-level waters would be 252 cm, 284 cm, and 308 cm for return periods of 20, 50, and 100 years, respectively (Table 5).

Table 5. Estimated water elevations (cm) for different return periods (Boljkovac).

No.	Distribution	Period (no. datasets)	Return period						
			2	10	20	50	100	200	500
1.	**Normal**	**1996–2022 (n = 27)**	**125**	**222**	**242**	**265**	**279**	**292**	**307**
		Without 2017 (n = 26)	144	193	207	223	233	242	252
		Difference	19	29	35	42	46	50	55
2.	**Lognormal**	**1996–2022 (n = 27)**	**143**	**229**	**261**	**302**	**332**	**362**	**399**
		Without 2017 (n = 26)	138	209	235	268	293	314	342
		Difference	5	20	26	34	39	48	57
3.	**Gamma**	**1996–2022 (n = 27)**	**146**	**225**	**252**	**284**	**308**	**330**	**356**
		Without 2017 (n = 26)	141	195	212	233	248	260	280
		Difference	5	30	40	51	60	70	76
Max. difference		1996–2022 (n = 27)	21	7	19	37	53	70	92
Max. difference		Without 2017 (n = 26)	6	16	28	45	60	72	90

Oskoruš et al. (2018) performed a statistical analysis of high water levels at the Boljkovac hydrological station for the series 1996–2016 (n = 21) and 1996–2017 (n = 22) using normal and log-normal distributions. By comparing the results from 2018 and our work for different series lengths, the highest water levels were observed in the series 1996–2017 (n = 22). With a normal distribution, the 50-year and 100-year water levels were approximately 20 cm higher in the series 1996–2017 (n = 22) than in the series 1996–2022 (n = 27). With a log-normal distribution, the series 1996–2017 (n = 22) had water levels that were approximately 30–40 cm higher than those of the series 1996–2022 (n = 27). The series 1996–2022, without 2017, had the lowest statistical water levels (n = 26). Statistically the longest possible series should always be considered.

The direct impact of extreme flooding on the results of the statistical analysis was previously quantified, which was best reflected in the results of the

series with 26 or 27 sets. The calculated water levels are shown in Fig. 10. The abscissa shows the returns for periods ranging from 2 to 500 years, whereas the ordinate shows the calculated water levels (cm). Therefore, the presented results confirm that when applying statistical analysis to high–level waters, the input data are important. Extreme situations that occur more frequently significantly influence the determination of characteristic hydrological quantities. Furthermore, they directly influence the selection of relevant hydrological parameters when sizing hydrotechnical facilities, including the height of embankments that protect the population from floods along rivers and estuaries.

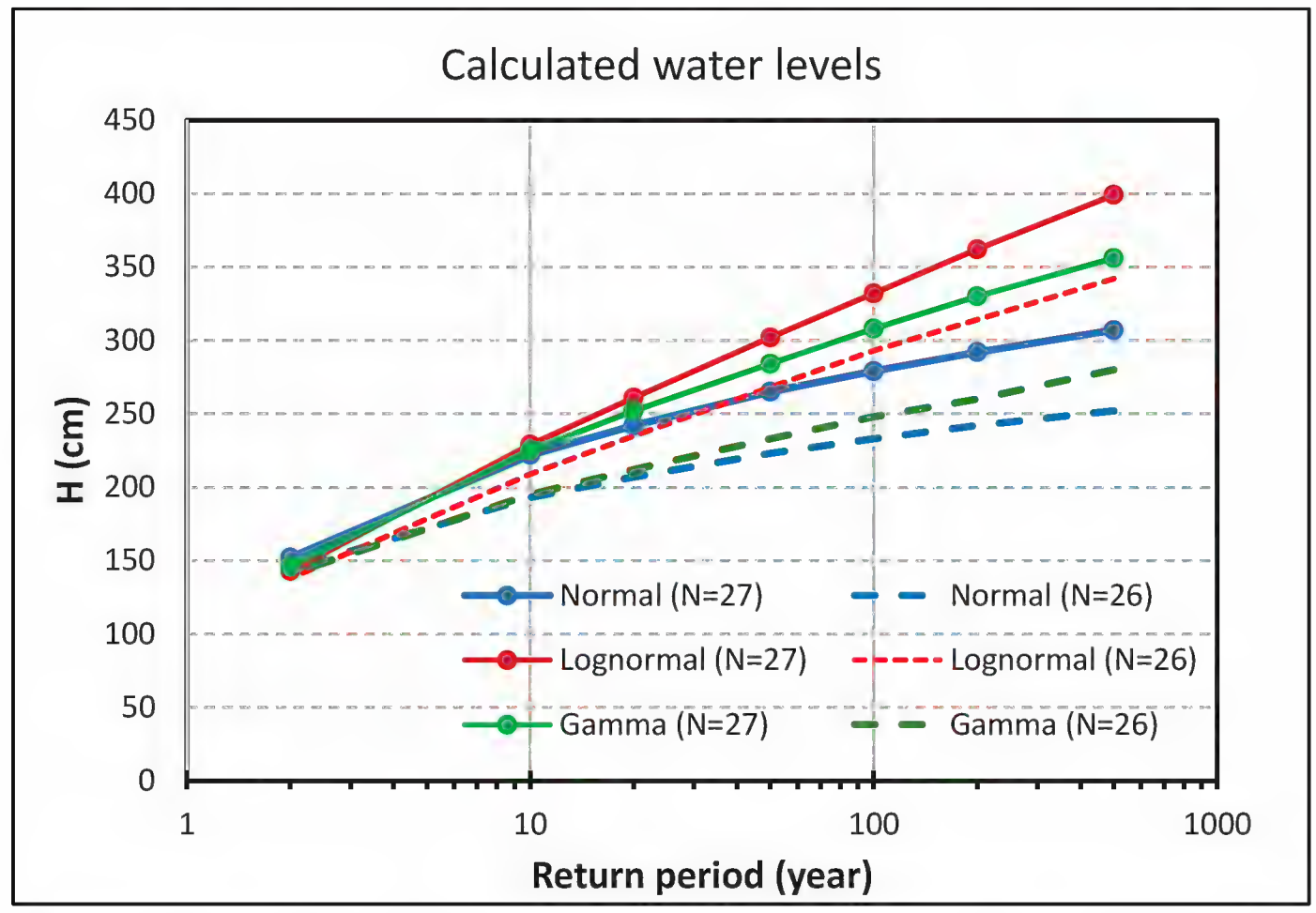

Figure 10. Comparison of calculated water levels for two series: a) 1996–2022 (n = 27) and b) the same period without 1997 (n = 26).

Based on the calculated high water levels, the associated discharges were determined using the discharge curve for the Boljkovac station. When we examine the estuary downstream of this watercourse, it is precisely the inflow of freshwater that presents an upstream boundary condition. Table 6 lists the flows of high water for return periods of 20, 50, and 100 years, which are typically considered in the design of hydrotechnical facilities. The calculated flows varied with an increase in the return period, which confirms the proportional relationship between the return period and the unreliability of the estimate. At the 100-year high water, the flow varied from 79 m^3/s (normal distribution) to 101 m^3/s (log-normal distribution), with a difference of approximately 20%. Comparing the length of the series and the water level, the series without extreme flooding (n = 26) yielded smaller flows. For a 100-year return period, flows amount from 60 to 85 m^3/s (n = 26), which is a decrease in flow from 16 to 29% compared to the longer series, depending on the selected distribution. This is a relatively large difference in the results, particularly because the input arrays in this case differ by only one term (n = 26 or 27). As stated earlier with regard to the water level, considering the results of the K–S test, we consider the Gamma distribution to be relevant. Therefore, the corresponding flows were

Table 6. Discharges (m^3/s) corresponding to high waters for different return periods.

No.	Distribution	Period (no. datasets)	Return period		
			20	50	100
1.	**Normal**	**1996–2022 (n = 27)**	**64**	**73**	**79**
		Without 2017 (n = 26)	49	56	60
		Difference	15	17	19
2.	**Lognormal**	**1996–2022 (n = 27)**	**72**	**89**	**101**
		Without 2017 (n = 26)	61	74	85
		Difference	11	15	16
3.	**Gamma**	**1996–2022 (n = 27)**	**67**	**81**	**92**
		Without 2017 (n = 26)	51	60	66
		Difference	16	21	26
Max. difference		1996–2022 (n = 27)	8	16	22
Max. difference		Without 2017 (n = 26)	12	18	25

67, 81, and 92 m^3/s for return periods of 20, 50, and 100 years, respectively. When applying statistical analyses, numerous other distributions can be used, particularly those common in hydrology. In doing so, even greater scattering of results can be expected, depending on the number of selected distributions.

The results indicate that statistical analysis is useful for water management, particularly in the design of hydrotechnical structures. However, the procedure for determining relevant hydrological quantities is complex and ambiguous. Continuous validation with the widest possible analysis of all available climatic, hydrological, and other parameters is required, to define runoff processes as precisely as possible. However, it should be emphasized that, apart from the application of probability theory itself, experience from practice is also important when analyzing extreme events.

Consequences of floods

The main object of flood defense in this area is an embankment built along the bed of the Miljašić jaruga, on the eastern side of the salt pan basin. The embankment was built in the middle of the 20th century as part of the works to modernize the salt works. In the past period, from the construction of the embankment until today, two instances of embankment damage were recorded in 1986 and 2017. For the event from 1986, with the highest recorded daily precipitation in Zadar, there were no hydrological measurements of this watercourse; therefore, it was difficult to conduct an appropriate analysis. Therefore, this study elaborated on the 2017 event in detail. As stated earlier, during the 2017 flood, the embankment overflowed with floodwaters. Minor or major damage was recorded over almost the entire length of the embankment (approximately 700 m). Part of the embankment with a length of approximately 50 m was completely destroyed by floodwater. (Fig. 11).

This flood significantly damaged two historically valuable bridges in the area of Nin, where apart from extremely large amounts of water, their partial collapse was also influenced by the reduced flow rate due to the rise in sea level since they were built. Damages to roads, beaches, numerous residential and commercial buildings were recorded. The greatest damage to economic facilities was caused by the salt works, because all pools were flooded and contaminated by the flow of torrential water.

Figure 11. Embankment damage during flooding, view downstream (Photo: I. Peša).

Rehabilitation post flood event

After the flood, the rehabilitation of the existing embankment began. All damage was repaired, and a new embankment made of clay was constructed on the affected section. The projected width of the crown was 2.5 m, with the adopted height of the crown being 3.0 m above sea level (Fig. 12), a figure calculated to be sufficient to receive a 100-year high water event. According to the results of the statistical analysis, all three distributions indicate that the 2017 flood event had a return period significantly longer than 100 years. However, it is common for the reconstruction or construction of new flood defense facilities in rural or smaller urban areas to be designed for high water return periods of up to 100 years (Ljubenkov and Papić 2015). Our previous experience in Dalmatian catchments and the current issue of climate change indicate that extreme events are occurring more frequently and with greater intensity than before. Therefore, we are likely to continue facing these challenges (Oskoruš et al. 2018; Ljubenkov et al. 2023).

Flood risk management recommendations

One possible measure to protect estuaries from fluvial floods is the construction of appropriate retention, barriers to calm the flow, and prevention of sedimentation or flood zones in the catchment areas. Thus, the Rašinovac retention is planned for the Miljašić jaruga, which would be located approximately 3.2 km upstream from the river mouth. In general, the high-quality management of catchment areas, that is, the planning and construction of appropriate facilities and systems for protection against the harmful effects of water, is important. Such tasks require good organization and engagement in several professions, such as spatial planning, climatology, and hydrology. It is likely that these phenomena will need to be addressed in the future.

Figure 12. Reconstructed embankment, view upstream (Photo: I. Peša).

Conclusion

The heavy rainfall in the northern part of Dalmatia (Croatia) in September 2017 and the Miljašić jaruga flooding event indicated the sensitivity of the estuary to extreme weather events. As shown in this study, extreme precipitation activated violent and torrential runoff in the entire catchment area (191 km^2) with the initiation and transfer of extreme amounts of sediment that caused great damage, particularly in the most downstream part of the catchment, estuary area, and town of Nin. The maximum flow at the most downstream hydrological station (Boljkovac) was estimated to be 112 m^3/s (water level H_{max} = 353 cm), whereas the volume of floodwater was approximately 10.6 million m^3. This was a typical flash flood with a significant rise in the water level over a relatively short time. Generally, owing to the extremely short time of occurrence and development of such events, it is difficult to provide adequate warnings or take timely preventative measures.

Extreme precipitation is expected to occur more often and at increasingly pronounced intensities owing to the influence of climate change. Therefore, it is important to conduct an appropriate analysis of such events to quantify runoff processes as precisely as possible. Depending on the characteristics of the catchment area, the timescale (duration) of precipitation that leads to large floods can range from a few tens of minutes to several days or months. Surface and underground water runoff processes, and their interactions, are particularly complex in karst areas. Quantifying extreme floods requires extensive analysis of various input data, from climatic and hydrological data, as well as numerous others that affect water circulation (geological and hydrogeological data, land use, and urbanisation). This study shows that input data for the assessment of relevant hydrological parameters are important. Considering the obvious climatic variations and changes, the hydrological bases used for designing hydrotechnical systems should be updated and validated as frequently as possible.

Based on the hydrological analyses, it is possible to design a protection system against the harmful effects of water. It is important to prepare infrastructure systems that are as resistant as possible to natural hazards, particularly in areas where non-resilience has already been established and in areas that have not previously experienced such events. The flood in the areas of Zadar and Nin

in 2017 damaged numerous infrastructural, residential, and commercial buildings amounting to tens of millions of Euros. This study quantified the basic meteorological and hydrological parameters that led to the historic flood and analyzed the obtained results, which showed great variability depending on the data used, length of the series, and calculation methodology. Such an approach is necessary in engineering practice and can be used for other similar systems such as estuaries and fluvial floods.

Additional information

Conflict of interest

The authors have declared that no competing interests exist.

Ethical statement

No ethical statement was reported.

Funding

No funding was reported.

Author contributions

All authors have contributed equally.

Author ORCIDs

Igor Ljubenkov https://orcid.org/0009-0005-7473-5880
Jovan Papić https://orcid.org/0000-0002-2952-302X

Data availability

All of the data that support the findings of this study are available in the main text.

References

Bevacqua E, Maraun D, Vousdoukas MI, Voukouvalas E, Vrac M, Mentaschi L, Widmann M (2019) Higher probability of compound flooding from precipitation and storm surge in Europe under anthropogenic climate change. Science Advances 5: 1–8. https://doi.org/10.1126/sciadv.aaw5531

Bonacci O (1987) Karst Hydrology with special references to the Dinaric karst. Springer-Verlag, Berlin, 184 pp. https://doi.org/10.1007/978-3-642-83165-2

Bonacci O (2015) Karst hydrogeology/hydrology of Dinaric chain and isles. Environmental Earth Sciences 74(1): 37–55. https://doi.org/10.1007/s12665-014-3677-8

Bonacci O, Ljubenkov I, Roje-Bonacci T (2006) Karst flash floods: an example from the Dinaric karst (Croatia). Natural Hazards and Earth System Science 6: 195–203. https://doi.org/10.5194/nhess-6-195-2006

Camarasa-Belmonte AM (2016) Flash floods in Mediterranean ephemeral streams in Valencia Region (Spain). Journal of Hydrology 541(A): 99–115. https://doi.org/10.1016/j.jhydrol.2016.03.019

DHMZ (2008) Climate atlas of Croatia. Zagreb.

Drew JH, Glen AG, Lawrence, Leemis LM (2000) Computing the cumulative distribution function of the Kolmogorov–Smirnov statistic. Computational Statistics & Data Analysis 34(1): 1–15. https://doi.org/10.1016/S0167-9473(99)00069-9

Harrison LM, Coulthard TJ, Robins P, Lewis M (2021) Sensitivity of estuaries to compound flooding. Estuaries and Coasts 45: 1250–1269. https://doi.org/10.1007/s12237-021-00996-1

IPCC (2023) Climate Changes: Synthesis Report. Geneva.

Jourde H, Lafare A, Mazzilli N, Belaud G, Neppel L, Dorfliger N, Cernesson F (2014) Flash flood mitigation as positive consequence of anthropogenic forcing on the groundwater resource in karst catchment. Environmental Erath Sciences 71: 573–583. https://doi.org/10.1007/s12665-013-2678-3

Kresic N (2013) Water in Karst: Management, Vulnerability and Restoration. McGraw-Hill, New York, 708 pp.

Lu W, Tang L, Yang D, Wu H, Liu Z (2022) Compounding effects of fluvial flooding and storm tides on coastal flooding risk in the coastal-estuarine region of Southeastern China. Atmosphere 13(238): 1–17. https://doi.org/10.3390/atmos13020238

Ljubenkov I, Haddout S (2024) Hydrodynamic modelling of a stratified estuary: the example of the Neretva River (Croatia). Marine Georesources & Geotechnology 42(1): 14–25. https://doi.org/10.1080/1064119X.2022.2147110

Ljubenkov I, Papić J (2015) Flooding of regulated riverbank: causes and protection solutions. In: Winter MG (Ed.) XVI European Conference on Soil Mechanics and Geotechnical Engineering, Edinburgh, Scotland.

Ljubenkov I, Peša I, Papić J (2023) Analysis of the River Zrmanja flood waters in Obrovac (Croatia). In: Petkovski Lj (Ed.) 13th Conference on water economy and hydrotechnics, Skopje, North Macedonia.

Lóczy D, Czigány S, Pirkhoffer E (2012) Flash Floods Hazards. In: Muthukrishnavellaisamy K (Ed.) Studies on Water Management Issues. InTech Open, 27–52. https://doi.org/10.5772/28775

Marechal JC, Ladouche B, Dorfliger N (2008) Karst flash flooding in a Mediterranean karst, the example of Fontaine de Nimes. Engineering Geology 99(3–4): 138–146. https://doi.org/10.1016/j.enggeo.2007.11.013

Martín-Vide JP, Niñerola D, Bateman A, Navarro A, Velasco E (1999) Runoff and sediment transport in a torrential ephemeral stream of the Mediterranean coast. Journal of Hydrology 225(3–4): 118–129. https://doi.org/10.1016/S0022-1694(99)00134-1

Massey FJ (1951) The Kolmogorov-Smirnov Test for Goodness of Fit. Journal of the American Statistical Association 46(253): 68–78. https://doi.org/10.2307/2280095

Meslard F, Balouin Y, Robin N, Bourrin F (2022) Assessing the Role of Extreme Mediterranean Events on Coastal River Outlet Dynamics. Water 14(16): 2463. https://doi.org/10.3390/w14162463

Mimikou MA, Baltas EA, Tsihrintzis VA (2016) Hydrology and Water Resources Systems Analysis. CRC Press, Taylor and Francis Group, Boca Raton FL, 459 pp. https://doi.org/10.1201/9781315374246

Oskoruš D, Berbic J, Vujnovic T, Macek K (2018) Extreme Floods in Zadar and Nin (Croatia) September 11, 2017. In: Davolio S (Ed.) 11th HyMeX, Lecce, Italy.

Petroliagkis TI, Voukouvalas E, Disperati J, Bidlot J (2016) Joint probabilities of storm surge, significant wave height and river discharge components of coastal flooding events. Publications Office of the European Union, Luxembourg, 84 pp.